Effect of Fe doping on the magnetic properties of GdBaCo$_2$O$_{5.5-\delta}$

Yan-kun Tang and C. C. Almasan

Department of Physics, Kent State University, Kent, Ohio 44242, USA
(Received 5 December 2007; revised manuscript received 23 January 2008; published 5 March 2008)

A detailed magnetic study has been carried out for the Fe-doped GdBaCo$_{2-x}$Fe$_x$O$_{5.5-\delta}$ ($x=0$, 0.02, 0.05, 0.10, and 0.20) cobaltites. Fe doping enhances the high-temperature T ferromagnetism present in the Fe-free samples and it induces a second ferromagnetic order, which develops at a lower T. Also, the spin-state transition temperature shifts to higher T with increasing the Fe content. Phase separation provides a phenomenological interpretation of these magnetic behaviors.

PACS number(s): 75.50.Bb, 75.30.Cr, 61.05.cp

I. INTRODUCTION

Cobalt oxides have been extensively studied during the past 60 years because of their rich physical properties and their technological applications.[1–3] Recently, a great deal of experimental effort has been made toward the study of REBaCo$_2$O$_{5.5-\delta}$, in which RE is a trivalent rare earth and the oxygen content δ varies from -0.5 to 0.5. Many interesting behaviors, such as giant magnetoresistance, large Seebeck coefficient, charge ordering, spin blockade, metal-insulator transition, and metamagnetic transformation, have been observed in these compounds.[4–15]

Because the oxygen content δ determines the mean valence and coordination of the Co ions, it plays a key role in the magnetic and transport properties of these compounds. REBaCo$_2$O$_5$ ($\delta=0.5$) contains corner-linked CoO$_5$ square pyramids as principal building units. It displays charge and orbital ordering, occurring in a G-type antiferromagnetic (AFM) structure.[7,16,17] In REBaCo$_2$O$_6$ ($\delta=-0.5$), Co^{3+} and Co^{4+} are present in the same amount and a cubic perovskite structure is obtained with CoO$_6$ octahedral building units.[18] For REBaCo$_2$O$_{5.5}$ ($\delta=0$), the valence of all Co ions is 3+. The Co^{3+} ions are located in alternating layers of CoO$_5$ pyramids and CoO$_6$ octahedra. At low temperatures, Co^{3+} adopts the intermediate spin (IS) state $t_{2g}^5 e_g^1$ in the pyramids and the low spin (LS) state $t_{2g}^6 e_g^0$ in the octahedra. The LS state of Co^{3+} in the octahedra changes at high temperatures to the high spin (HS) state $t_{2g}^4 e_g^2$, accompanied by a metal-insulator transition.[9–11,15,19]

Furthermore, Taskin *et al.*[10,12,14] found a remarkable uniaxial anisotropy of the Co spins along the oxygen chain, i.e., along the a axis of GdBaCo$_2$O$_{5.5-\delta}$ single crystals. The magnetic structure appears to be composed of weakly coupled ferromagnetic (FM) ladders. There is an AFM ground state at low temperatures because the interaction between different FM ladders is antiferromagnetic. However, the strength of interladder coupling is weak so that switching from the AFM order to the FM one can be induced easily. Thus, the magnetic behavior of REBaCo$_2$O$_{5.5-\delta}$ can easily be affected by temperature, magnetic field, and oxygen doping due to the delicate balance between FM and AFM interactions. In addition, a few percent variation in the oxygen content induces phase separation in this system.[14]

The magnetic properties of transition-metal oxides are mainly determined by the magnetic exchange interaction between the transition-metal ions. The replacement of one transition-metal ion by another one could have a great impact on their magnetic properties. For example, Fe doping greatly suppresses both the double-exchange interaction and the ferromagnetism in manganites.[20] Recently, several groups have reported on the doping effect of transition-metal ions on the magnetic properties of REBaCo$_{2-x}$M$_x$O$_{5.5-\delta}$ (RE=Tb,Eu; $M=$Zn,Cu,Fe).[21–24] Increased ferromagnetism at low temperatures, ultrasharp magnetization multisteps, and decreased oxygen content have all been observed in these systems.

In this paper, we report on the magnetic properties of GdBaCo$_{2-x}$Fe$_x$O$_{5.5-\delta}$. The magnetization data reveal that a second ferromagnetic order develops at low temperatures as a result of Fe doping, while the first ferromagnetic order (also present in the Fe-free samples) shifts to higher temperatures with increasing Fe doping. Additionally, the spin-state transition, present in the Fe-free samples, shifts to higher temperatures with increasing Fe doping. We explain these findings in the framework of phase separation triggered by Fe doping.

II. EXPERIMENTAL DETAILS

Polycrystalline GdBaCo$_{2-x}$Fe$_x$O$_{5.5-\delta}$ ($x=0$, 0.02, 0.05, 0.10, and 0.20) samples were prepared by the solid state reaction method. A stoichiometric mixture of Gd$_2$O$_3$, BaCO$_3$, Co$_3$O$_4$, and Fe$_2$O$_3$ powders was well grinded and calcinated twice, first at 800 °C and then at 950 °C for 24 h each. The resulting powder was then pressed into pellets and sintered at 1100 °C for 24 h. After a regrinding of the resulting pellets, the compression and sintering processes were repeated one more time. X-ray diffraction (XRD) patterns were collected at room temperature with a Rigaku x-ray diffractometer with Cu $K\alpha$ radiation. The magnetization measurements were performed using a commercial Quantum Design superconducting quantum interference device magnetometer.

III. RESULTS AND DISCUSSION

Figure 1 shows the XRD patterns of the GdBaCo$_{2-x}$Fe$_x$O$_{5.5-\delta}$ samples for five different Fe dopings between $x=0$ and $x=0.20$. All the XRD patterns can be indexed using an orthorhombic symmetry. No appreciable impurity peaks have been observed for these Fe-doped samples. The XRD patterns reveal that all the samples are single phase
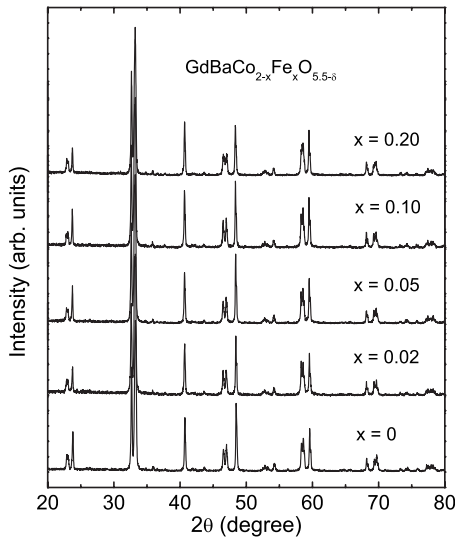
FIG. 1. X-ray diffraction patterns of $GdBaCo_{2-x}Fe_xO_{5.5-\delta}$ ($x=0$, 0.02, 0.05, 0.10, and 0.20) samples measured at room temperature.

within the resolution of the x-ray diffractometer, with an orthorhombic perovskite structure.

The dependence of the structural parameters on the Fe concentration x is plotted in Fig. 2. Notice the slight variation of the structural parameters with Fe doping. The lattice parameters b and c and the unit-cell volume V slightly increase with increasing Fe doping. However, the lattice parameter a tends to decrease as x increases. Kopcewicz et al.[21] have shown through a Mössbauer spectroscopy study on $TbBaCo_{2-x}Fe_xO_{5.5-\delta}$ that the Fe^{3+} ions preferentially adopt a HS state at the pyramidal sites. In addition, the radius of 0.645 Å of the HS state of the Fe^{3+} ions is larger than the radius of 0.56 Å of the IS state of the Co^{3+} ions at the pyramidal sites,[25] which are the ones replaced by the Fe^{3+} ions in the doping process. This explains the increase in the unit-cell volume of $GdBaCo_{2-x}Fe_xO_{5.5-\delta}$ with increasing the amount of Fe^{3+} substituted for Co^{3+}.

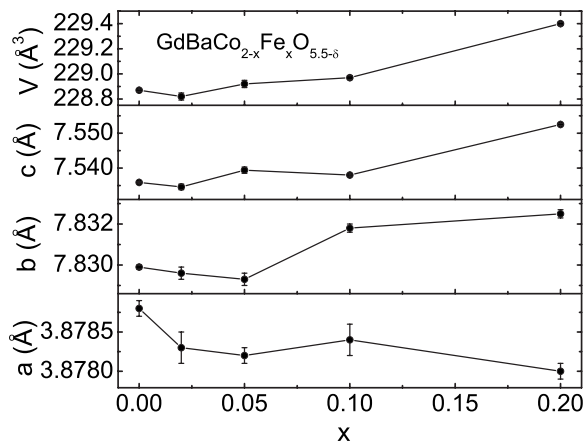The temperature dependence of the magnetization M measured in increasing the temperature after field cooling the

FIG. 2. Dependence of the structural parameters, i.e., the lattice parameters a, b, and c and the unit-cell volume V, on the Fe concentration x in $GdBaCo_{2-x}Fe_xO_{5.5-\delta}$.

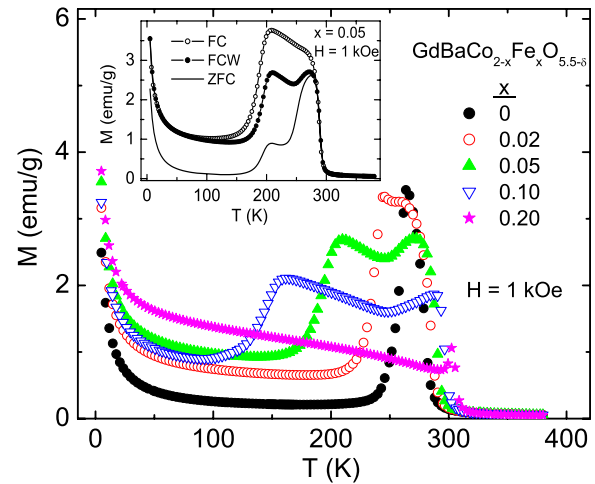FIG. 3. (Color online) Temperature T dependence of the field-cooled magnetization M for $GdBaCo_{2-x}Fe_xO_{5.5-\delta}$ ($x=0$, 0.02, 0.05, 0.10, and 0.20) measured in increasing the temperature (FCW) after field cooling the sample in an applied magnetic field of 1 kOe. Inset: M vs T for the $x=0.05$ sample measured using the following three different protocols: cooling the sample in zero field, followed by applying the desired H, and measuring $M(T)$ in increasing T (ZFC protocol); field cooling the sample and measuring $M(T)$ in increasing T (FCW protocol); field cooling the sample and measuring $M(T)$ while cooling it (FC protocol).

sample [field-cooled warming (FCW)] in 1000 Oe is shown in Fig. 3 for the five Fe-doped samples. The Fe-free sample displays a magnetization peak around 265 K. This magnetization peak has previously been reported for $GdBaCo_2O_{5.5}$ by other groups,[5,8,15] as being the result of a paramagnetic (PM) to FM transition around 290 K and a FM to AFM transition around 240 K. We estimate that $\delta \approx 0$ for the present Fe-free sample based on the fact that the above two transition temperatures reported for $GdBaCo_2O_{5.5}$ are very close to the ones shown here for the Fe-free sample.

A small replacement of Co with Fe leads to a remarkable change in the FCW magnetization curves of $GdBaCo_{2-x}Fe_xO_{5.5-\delta}$. Specifically, a second magnetization peak appears in the Fe-doped samples, which shifts to lower temperatures with increasing Fe doping (see Fig. 3). In contrast, the first magnetization peak displays a small shift to higher temperatures with Fe doping. These two behaviors suggest an enhanced ferromagnetism both at low temperatures as well as at high temperatures.

Due to the hysteretic nature of these samples, the measurement history modifies the $M(T)$ curves. The inset of Fig. 3 illustrates this for the $x=0.05$ sample. The three protocols applied here are (i) cooling the sample in zero field, followed by applying the desired H, and measuring $M(T)$ in increasing T [zero field-cooled (ZFC) protocol], (ii) field cooling the sample and measuring $M(T)$ in increasing T (FCW protocol), and (iii) field cooling the sample and measuring $M(T)$ while cooling it (FC protocol). Notice that both magnetization peaks are enhanced when the measuring protocol changes from ZFC to FCW and then further to FC. The magnetization is the largest in the FC protocol and the lowest in the ZFC protocol since the FC protocol is the one which takes the
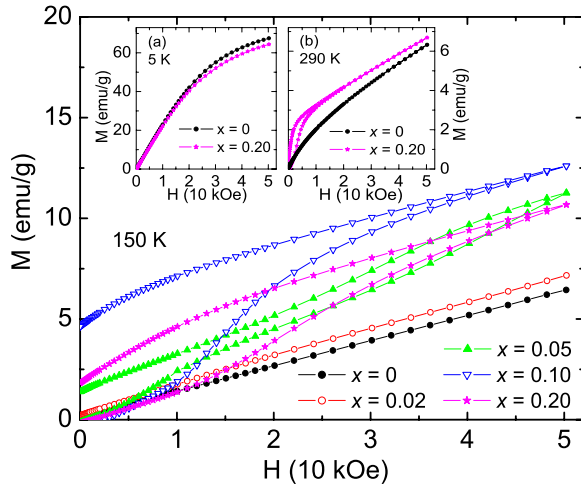
FIG. 4. (Color online) Magnetization M vs applied field H of GdBaCo$_{2-x}$Fe$_x$O$_{5.5-\delta}$ (x=0, 0.02, 0.05, 0.10, and 0.20) measured at 150 K. Inset: M vs H of the GdBaCo$_{2-x}$Fe$_x$O$_{5.5-\delta}$ samples with x =0 and 0.20 measured at (a) 5 K and (b) 290 K.

system through a sequence of equilibrium states while the ZFC protocol gives rise to the highest degree of frustration in the spin system. This behavior is typical for all the Fe-doped samples.

The magnetic state of the GdBaCo$_{2-x}$Fe$_x$O$_{5.5-\delta}$ samples has been further investigated through $M(H)$ measurements at different temperatures, in which the sample is zero field cooled to the desired T and then $M(H)$ is measured first in increasing H up to 50 kOe and then in decreasing H to 0 Oe. The $M(H)$ curve measured at 5 K shows a typical paramagnetic behavior for all samples [see inset (a) of Fig. 4; for clarity, only the $M(H)$ curves of the x=0 and 0.20 samples are shown]. This is consistent with the rapid growth of the magnetization below 40 K in the $M(T)$ curves (see Fig. 3). The paramagnetic moment of Gd contributes to the large value of the magnetization.

The linear $M(H)$ curves of the x=0 and 0.02 samples measured at 150 K (see Fig. 4) represent the paramagnetism of the Co ions. For the samples with a larger amount of Fe, ferromagnetic behavior appears evidenced by hysteresis and remanent magnetization (see Fig. 4). This magnetic behavior revealed in the $M(H)$ curves shows that the second peak observed in the $M(T)$ curves at lower T (see Fig. 3), indeed, reflects a second ferromagnetic order which develops at these lower temperatures.

At 290 K [the temperature around which there is a PM to FM transition in $M(T)$ as shown by the high T peak in Fig. 3], no hysteresis is observed for lower amounts of Fe doping although the $M(H)$ curves are not completely linear [see inset (b) of Fig. 4], which indicates the presence of short range ferromagnetic interactions. Nevertheless, the hysteresis in $M(H)$ for the x=0.20 sample shows the presence of ferromagnetism at this T, which is the result of the shift of the $M(T)$ peak, hence the FM transition temperature, to higher T with Fe doping (see Fig. 3).

All the $M(H,T)$ data presented above show the presence of a second FM order at low T in the Fe-doped samples, in

addition to the high-temperature FM order present in all the samples, including the Fe-free samples (see Figs. 3 and 4). Since no new chemical phase was detected within the resolution of the x-ray diffractometer (see Fig. 1), these magnetic results indicate that Fe doping leads to phase separation in GdBaCo$_{2-x}$Fe$_x$O$_{5.5-\delta}$, with the Fe-rich regions giving rise to the low-temperature FM order and the Fe-free regions giving rise to the high-temperature FM order. Both FM orders originate from the coupling between neighboring ladders in CoO$_5$ pyramidal layers. This weak coupling depends on the thermally excited Co^{2+} and Co^{4+} and competes with the AFM superexchange interaction.[10] Both magnetic field and temperature can affect these two FM orders, giving rise to the observed metamagnetic behavior (see Fig. 4) and to the history-dependent magnetic response (see Fig. 3). At the same time, as shown below, Fe doping also affects the magnetic behavior of the Fe-free regions. Previously, phase separation has been observed in GdBaCo$_2$O$_{5.5-\delta}$ as a result of the variation in the oxygen content.[14]

We note that a second FM order along the a axis has also been observed at low T in detwinned Tb$_{0.9}$Dy$_{0.1}$BaCo$_2$O$_{5.5}$ single crystals, which has been associated with the partial lack of compensation of the AFM order.[26] However, this small FM component can only be observed in detwinned single crystals because of the unidirectional anisotropy. Also, it does not depend on Dy doping. Hence, the second FM order reported here in polycrystalline samples, which varies systematically with Fe doping, is not a result of the partial lack of compensation of the AFM order.

In the study of the effect of iron doping on the properties of TbBaCo$_2$O$_{5.5}$, both Mössbauer spectroscopy and thermogravimetric analysis have revealed that an increase in the Fe content leads to a decrease in the oxygen content.[21] Considering the very similar structure of TbBaCo$_2$O$_{5.5}$ and GdBaCo$_2$O$_{5.5}$, it is also likely that an increase in the Fe content in the Fe-rich regions leads to a decrease in the oxygen content of these regions. Furthermore, the phase diagram of GdBaCo$_2$O$_{5.5-\delta}$ shows that a decrease in the oxygen content gives rise to a decrease in both PM-FM and FM-AFM transition temperatures.[14] This explains the shift of the low-temperature $M(T)$ peak (corresponding to the ferromagnetic order in the Fe-rich regions) to lower temperatures with increasing Fe doping. Beside the oxygen content, the exchange interaction between Co and Fe also affects the magnetic properties of the Fe-rich regions. According to the Goodenough-Kanamori rules,[27,28] an AFM superexchange interaction is expected for Fe^{3+}-O-Co^{2+} and Fe^{3+}-O-Co^{3+}. This interaction suppresses the ferromagnetism and decreases quickly the PM-FM transition temperature.

One could expect that the magnetic properties of the Fe-free regions are the same as the ones for the Fe-free samples. Nevertheless, this is not the case since Fe doping slightly shifts the high T magnetic transition, corresponding to the Fe-free regions, to higher temperatures (see Fig. 3). This shift can be explained as follows. Figure 2 shows that the unit-cell volume V of GdBaCo$_{2-x}$Fe$_x$O$_{5.5-\delta}$ slightly increases with increasing Fe doping. This expansion should mainly take place in the Fe-rich regions. As a result, compression takes place in the Fe-free regions because of the surrounding expansion of the Fe-rich regions. A consequence of this com-
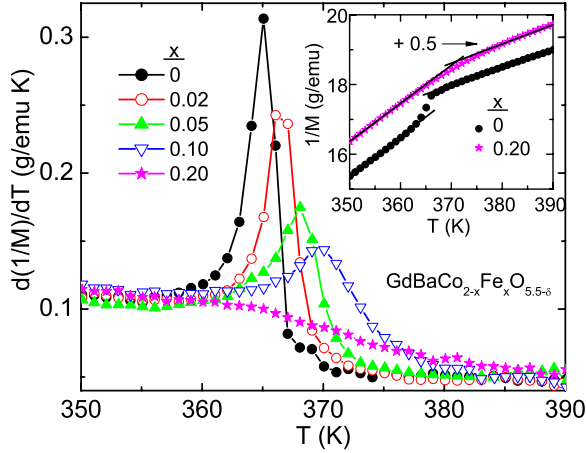
FIG. 5. (Color online) Derivative of the inverse magnetization $d(1/M)/dT$ for all measured samples. Inset: Temperature T dependence of inverse magnetization $1/M$ for the $GdBaCo_{2-x}Fe_xO_{5.5-\delta}$ samples with $x=0$ and 0.20. The $1/M$ for the $x=0.20$ sample are vertically offset by $+0.5$ g/emu for clarity.

pression on the magnetic properties of $GdBaCo_{2-x}Fe_xO_{5.5-\delta}$ is that the superexchange FM interaction between Co^{3+}-O-Co^{3+} is strengthened due to the shrinkage of the Co-O bond length. So the ferromagnetism is enhanced and the PM-FM transition temperature shifts to higher temperatures.

It has been found that the spin-state transition of the $REBaCo_2O_{5.5-\delta}$ compounds delicately depends on the rare earth and the oxygen content.[13] Here, we study the doping effect of transition-metal ions on the spin-state transition. For clarity, the inset of Fig. 5 only shows the $1/M(T)$ curves of the $x=0$ and 0.20 samples. Notice that there are two temperature regions in the $1/M(T)$ curves that can be linearly fitted and that the slope of the low T region ($350 \text{ K} \leq T \leq 360 \text{ K}$) is larger than the slope of the high T region ($380 \text{ K} \leq T \leq 390 \text{ K}$). Because all these samples are paramagnetic above 320 K, the decrease in the slope of $1/M(T)$ at high temperatures implies that the effective paramagnetic moment increases at these temperatures. That is, a transition from a LS state to a HS state takes place. This spin-state transition has been observed for all Fe-doped samples with $x \leq 0.20$.

Baran et al.[26] also observed a steplike change in $1/M(T)$ in the paramagnetic phase, near 340 K, of detwinned $Tb_{0.9}Dy_{0.1}BaCo_2O_{5.5}$ single crystals. They calculated the changes of the effective magnetic moments along the three crystallographic axes and found that these changes are anisotropic. This indicates that these changes of the magnetic moments at 340 K do not correlate to the spin-state transition. Nevertheless, the presence of the spin-state transition in $GdBaCo_2O_{5.5-\delta}$ has been established through both Curie-Weiss fitting of the paramagnetic susceptibility in detwinned $GdBaCo_2O_{5.5-\delta}$ single crystals,[14] as well as through ultrahigh resolution synchrotron diffraction data on $GdBaCo_2O_{5.5}$, which show that the spin-state transition is the driving force for the metal-insulator transition.[9]

The two slopes of $1/M$ vs T give the moment of $GdBaCo_{2-x}Fe_xO_{5.5-\delta}$ below and above the spin-state transition temperature T_s, respectively, by fitting these data with a Curie-Weiss law. After subtracting the moment of Gd ($\mu_{Gd}=8.0\mu_B$), the average spin moment per unit cell is $2.05\mu_B$ for $T < T_s$ and $3.91\mu_B$ for $T > T_s$ for the $x=0$ sample and $1.89\mu_B$ for $T < T_s$ and $3.12\mu_B$ for $T > T_s$ for the $x=0.20$ sample. As a result of the spin-state transition, the spin moment per unit cell increases by $1.86\mu_B$ and $1.23\mu_B$ for the $x=0$ and $x=0.20$, respectively. The fact that the increase in the spin moment at T_s is not the same for the $x=0$ and $x=0.20$ samples shows that the amount of Co ions which undergo the spin-state transition decreases with Fe doping, most likely because the number of Co ions in octahedral positions decreases due to a decrease in oxygen amount in the Fe-rich regions. Therefore, this indicates that the spin-state transition takes place mainly in the Fe-free regions.

Also, notice the sharp steplike change in $1/M(T)$ in the spin-state transition region of the $x=0$ sample (see the inset of Fig. 5). This steplike increase in $1/M(T)$ is not due to the spin-state transition itself because the spin state changes from the LS state to HS state with increasing T in the spin-state transition region, while this steplike increase in $1/M(T)$ would give rise to a decrease of the moment. This increase in $1/M(T)$ is also not related to sample quality because it has also been observed in single crystals of $GdBaCo_2O_{5.5}$ (Ref. 14). Using the local spin-density approximation $+U$ method, Kwon et al.[29] have found that the orbital moment of Co^{3+} is only partially quenched in $YBaCo_2O_5$ at low temperatures. The orbital moment originates from the localized nature of the Co $3d$ electrons. Thus, a possible explanation for the sharp decrease in $M(T)$ in the spin-state transition region is that at T_s, the orbital moment is suppressed due to the fact that the Co $3d$ electrons are delocalized. Indeed, it has been shown that the spin-state transition is accompanied by a metal-insulator transition.[5] Therefore, in the LS state (low T), the conduction electrons are localized, while in the HS state (high T), the conduction electrons are delocalized.

The steplike decrease in $M(T)$ becomes weaker with increasing Fe doping and disappears for the $x=0.20$ sample. This is also a result of the fact that the spin-state transition, hence metal-insulator transition, takes place mainly in the Fe-free regions. Hence, the amount of Co ions present in these regions, which contribute to the steplike decrease in $M(T)$, is strongly reduced with Fe doping.

Figure 5 displays the slopes of the $1/M$ vs T data for different Fe dopings. The constant slopes at low and high temperatures reflect the magnetic moment in the LS state and HS state, respectively. We define the spin-state transition temperature $T_s \equiv (T_1+T_2)/2$, where T_1 and T_2 are the beginning and ending temperatures of the spin-state transition, respectively. For $x=0$, 0.02, 0.05, 0.10, and 0.20, $T_s=365$, 366, 368, 370, and 372 K, respectively. Hence, the spin-state transition temperature increases with increasing Fe doping. This can be explained based again on the compression that takes place in the Fe-free regions because of the surrounding expansion of the Fe-rich regions. Namely, the compression of the CoO_6 volume, due to the shrinkage of the Co-O bond length, leads to an increase in the crystal-field splitting energy (Δ_{CF}), as shown by Fita et al.[30] in their study of the external pressure effect on the spin state of $La_{1-x}M_xCoO_3$ ($M=Ca, Sr$). The balance between Δ_{CF} and the Hund ex-

change energy (J_H) determines the spin-state transition. Therefore, an increase in Δ_{CF} with increasing Fe doping implies that a larger thermal energy is needed to excite the Co^{3+} ions from the LS state to the HS state. As a result, the spin-state transition temperature shifts to higher temperatures in the Fe-free regions with increasing Fe doping.

IV. CONCLUSION

In summary, we have systematically studied the Fe doping effect on the magnetic properties of Fe-doped $GdBaCo_2O_{5.5-\delta}$. Fe doping leads to phase separation into Fe-rich and Fe-free regions and, as a consequence, to two magnetic phases. The Fe-rich regions are responsible for the low-temperature $M(T)$ peak, which shifts to lower temperatures with increasing the Fe content. This shift is due to the decrease in the oxygen content with increasing Fe doping and the presence of the AFM Fe-Co superexchange interaction in the Fe-doped samples. The high-temperature $M(T)$ peak (corresponding to the Fe-free regions) and the spin-state transition temperature shift to higher temperatures with Fe doping as a result of the slight compression of the Fe-free regions with Fe doping.

ACKNOWLEDGMENT

[1] W. C. Koehler and E. O. Wollan, J. Phys. Chem. Solids **2**, 100 (1957).

[2] G. Briceño, H. Chang, X. Sun, P. G. Schultz, and X. D. Xiang, Science **270**, 273 (1995).

[3] K. Takada, H. Sakurai, E. Takayama-Muromachi, F. Izumi, R. A. Dilanian, and T. Sasaki, Nature (London) **422**, 53 (2003).

[4] C. Martin, A. Maignan, D. Pelloquin, N. Nguyen, and B. Raveau, Appl. Phys. Lett. **71**, 1421 (1997).

[5] I. O. Troyanchuk, N. V. Kasper, D. D. Khalyavin, H. Szymczak, R. Szymczak, and M. Baran, Phys. Rev. Lett. **80**, 3380 (1998).

[6] Y. Moritomo, M. Takeo, X. J. Liu, T. Akimoto, and A. Nakamura, Phys. Rev. B **58**, R13334 (1998).

[7] T. Vogt, P. M. Woodward, P. Karen, B. A. Hunter, P. Henning, and A. R. Moodenbaugh, Phys. Rev. Lett. **84**, 2969 (2000).

[8] M. Respaud, C. Frontera, J. L. García-Muñoz, Miguel Ángel G. Aranda, B. Raquet, J. M. Broto, H. Rakoto, M. Goiran, A. Llobet, and J. Rodríguez-Carvajal, Phys. Rev. B **64**, 214401 (2001).

[9] C. Frontera, J. L. García-Muñoz, A. Llobet, and M. A. G. Aranda, Phys. Rev. B **65**, 180405(R) (2002).

[10] A. A. Taskin, A. N. Lavrov, and Y. Ando, Phys. Rev. Lett. **90**, 227201 (2003).

[11] A. Maignan, V. Caignaert, B. Raveau, D. Khomskii, and G. Sawatzky, Phys. Rev. Lett. **93**, 026401 (2004).

[12] A. A. Taskin and Y. Ando, Phys. Rev. Lett. **95**, 176603 (2005).

[13] S. Roy, I. S. Dubenko, M. Khan, E. M. Condon, J. Craig, N. Ali, W. Liu, and B. S. Mitchell, Phys. Rev. B **71**, 024419 (2005).

[14] A. A. Taskin, A. N. Lavrov, and Y. Ando, Phys. Rev. B **71**, 134414 (2005).

[15] C. Frontera, J. L. García-Muñoz, A. E. Carrillo, M. A. G. Aranda, I. Margiolaki, and A. Caneiro, Phys. Rev. B **74**, 054406 (2006).

[16] E. Suard, F. Fauth, V. Caignaert, I. Mirebeau, and G. Baldinozzi, Phys. Rev. B **61**, R11871 (2000).

[17] D. Akahoshi and Y. Ueda, J. Solid State Chem. **156**, 355 (2001).

[18] E. Suard, F. Fauth, and V. Caignaert, Physica B **276-278**, 254 (2000).

[19] F. Fauth, E. Suard, V. Caignaert, and I. Mirebeau, Phys. Rev. B **66**, 184421 (2002).

[20] K. H. Ahn, X. W. Wu, K. Liu, and C. L. Chien, Phys. Rev. B **54**, 15299 (1996).

[21] M. Kopcewicz, D. D. Khalyavin, I. O. Troyanchuk, H. Szymczak, R. Szymczak, D. J. Logvinovich, and E. N. Naumovich, J. Appl. Phys. **93**, 479 (2003).

[22] D. D. Khalyavin, A. M. Balagurov, A. I. Beskrovnyi, I. O. Troyanchuk, A. P. Sazonov, E. V. Tsipis, and V. V. Kharton, J. Solid State Chem. **177**, 2068 (2004).

[23] B. Raveau, Ch. Simon, V. Pralong, V. Caignaert, and F.-X. Lefèvre, Solid State Commun. **139**, 301 (2006).

[24] B. Raveau, Ch. Simon, V. Caignaert, V. Pralong, and F.-X. Lefèvre, J. Phys.: Condens. Matter **18**, 10237 (2006).

[25] R. D. Shannon, Acta Crystallogr., Sect. A: Cryst. Phys., Diffr., Theor. Gen. Crystallogr. **A32**, 751 (1976).

[26] M. Baran, V. I. Gatalskaya, R. Szymczak, S. V. Shiryaev, S. N. Barilo, G. L. Bychkov, and H. Szymczak, J. Phys.: Condens. Matter **17**, 5613 (2005).

[27] J. B. Goodenough, Phys. Rev. **100**, 564 (1955).

[28] J. Kanamori, J. Phys. Chem. Solids **10**, 87 (1959).

[29] S. K. Kwon, J. H. Park, and B. I. Min, Phys. Rev. B **62**, R14637 (2000).

[30] I. Fita, R. Szymczak, R. Puzniak, I. O. Troyanchuk, J. Fink-Finowicki, Ya. M. Mukovskii, V. N. Varyukhin, and H. Szymczak, Phys. Rev. B **71**, 214404 (2005).